Vol 1, Issue 1, pages ***High School Research Journal***

CONTROLLING COHERENCE IN THE PRODUCT CHANNEL FROM A DIRECT, UNI-MOLECULAR DISSOCIATION REACTION

Jason Getzler
Plainview-Old Bethpage John F. Kennedy High School, 50 Kennedy Drive, Plainview, New York 11803, 516-434-3125
Dr. Gail Richmond
Michiagn State Universtuiy, 620 Farm Lane, East Lansing, MI 48824, 517-432-4854, gailr@msu.edu

ABSTRACT

The critical transition from reactants to products occurs in less than a picosecond (10-12 s). Using an ultrafast femtosecond laser (10-15s), it is possible to further understand particle motion before, during, and after the chemical reaction transition. In this study, triiodide (I_3^-), a simply-structured ion often used because of its stability and efficiency, was subjected to femtosecond laser pulses (NIR and UV wavelengths) to analyze the molecular photodissociation dynamics on an ultrashort time scale (10-12 seconds or shorter). First, vibrational oscillations from diidoide previously reported were replicated via pump-probe spectroscopy to confirm validity of experimentation model. This was followed by innovative pulse shaping techniques to maximize peak oscillations produced by molecules. Oscillation periods were statistically analyzed to understand the dynamics (the movement and vibrations of molecules) undergone by the I_3^-, over increased time delay. It was demonstrated that vibrational oscillations in triiodide solution, when subjected to UV pulse shaping using the MIIPS system, show a ±1.0E2 variance in optimal parameters for maximized oscillatory amplitudes and undergo cooling effects as the reaction ensues. Taken together, these observations shed new light on the application of the theoretical laws of quantum mechanics in describing the experimental dynamics of diiodide and that excited-state diiodide oscillations can be controlled by UV light to potentially undergo wavepacket focusing in the product channel of chemical reactions.

Keywords: Femtosecond chemistry, Pump-probe spectroscopy, pulse shaping, triiodide, diiodide, photodissocation, product channel

INTRODUCTION

Controlling the dynamics of chemical reactions using ultrafast light can be extremely lucrative in the biotechnological, solar energy, and food industries [1-

3]. Moreover, the ability to control the stages of a reaction using laser pulses will add to our understanding of the dynamics of light-matter interactions at the molecular level, for molecules hit with ultrafast laser pulses alter electron distribution and trigger unusual chemical reactions [4]. While dynamics of such interactions are believed to be guided by the laws of quantum mechanics [5], the theoretical principles of quantum mechanics have yet to be widely applied to experimental testing [6]. With the presence of coherent control—that is, all molecules undergoing similar dynamics simulteanously, [7,8] —being a key concept of quantum theory, experimental analysis of such molecular motion would be a step in validation of theory application. In this study, high-energy, non-destructive femtosecond laser pulses are used to analyze the dynamics of light-matter interactions. This technology brings theoretical studies of light-matter interactions to the next level, featuring unprecedented accuracy and reproducibility in experimentally applying quantum theory to chemical reactions.

In this study, an in-depth analysis was conducted on triiodide (I_3^-), a simply-structured molecule [9] often utilized in dye-sensitized solar cells due to its stability and efficiency. Triiodide was subjected to shaped femtosecond (10^{-15}s) laser pulses (NIR and UV wavelengths) to analyze the dynamics between the molecules and light on an ultrashort time scale. This will also experimentally investigate the use of quantum mechanics theory to show how the product-channel diiodide molecules from the dissociation reaction can indeed absorb and emit photons at unique frequencies.

Femtosecond Chemistry

Non-linear optics is the field of study in which light-matter interactions in an applied electric field produce an amplitude in a nonlinear orientation to said field [10]. Through the use of lasers, scientists have been able to closely monitor such interactions between light and matter in a controlled environment [11,12]. A laser created by Peter Moulton at MIT in 1982 [12] that has the capacity to release pulses with a duration of several femtoseconds (10^{-15}seconds) [11] facilitates

such control and was a discovery that created new technology—ultrashort laser pulses [13]. This technology enables studies of the dynamics of molecules in great detail because these pulses are incredibly intense and yet non-destructive because of their brevity [14]. Furthermore, this technology can be adapted to study velocity of chemical reaction with high accuracy never achieved before.

Pump-Probe Spectroscopy

Pump-probe spectroscopy is often employed to study how laser light interacts with molecules. This technique includes two steps of laser pulse emission: the first pulse administered, the "pump" pulse, is a beam that excites the sample from the ground state; the second pulse, or the "probe" pulse, is released to interact with the molecules in the excited state, and thus monitors the changes in energy and photon transmission of the sample as a function of time [15]. A key component of this technique involves recording the time delay between the pump and probe pulses. If there is a large delay between the pulses' interactions with the sample, particles have the potential to emit the absorbed photons of light, and thus return to the ground state before receiving the probe pulse. A shorter delay suggests that particles are in the excited state upon interaction with the probe beam [16]. Additionally, a positive delay is defined as that the pump pulse interacts with the sample prior to the probe pulse, while a negative delay indicates the contrary [16]. Analysis of different stages of this process can be achieved using varying pulse emissions [17], including testing the absorption and emission of pulses at different frequencies that can ultimately lead to selecting the optimal experimentation parameters.

Pulse Shaping

While this pump-probe process alone has the ability to reveal much about molecular dynamics, further possibilities arise with the introduction of a pulse shaper to the system. Pulse

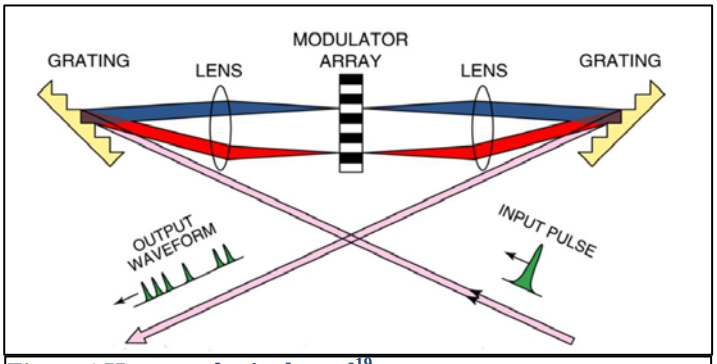

Figure 1 **How a pulse is shaped**[19]

shaping is a process initially implemented in the 1970s [18], during which an unaltered laser pulse (transform limited) is adapted to meet the specified parameters of an experiment. In this study, utilization of this process is being applied to UV pulses. Figure 1 depicts the process of pulse shaping. First, an input pulse hits the grating, which disperses the wave according to its component wavelengths. Then, the modulator array, controlled by the computer, alters the phase and intensity of the pulse [19]. Once they are recombined at the second grating, a variety of waves can be produced based off alteration completed during modulation. These alterations include reducing bandwidth, reducing background noise, compensating for dispersion effects, increasing number of waves, and instating higher order dispersion (where light is split into components by differing frequencies) [20,21]. Second order dispersion, also known as “chirp,” is of great significance since it increases or decreases the frequency of the pulse, thus decreasing dispersion effects upon interaction with matter [22]. While a plethora of pulse shaping characteristic methods exist, such as FROG (Frequency Resolved Optical Grating) and SPIDER (Spectral Phase Interferometry for Direct Electric Field Reconstruction), the optimal system is the pulse categorizer and shaper Multiphoton Intrapulse Interference Phase Scan (MIIPS) [21,23,24]. The MIIPS pulse shaper is considered the ideal choice because not only is it able to shape the pulse with the most accuracy (as per other pulse shapers), with a weighted .013 rad error [23], but it also has a broad spectral wavelength capability (400 nm-1500 nm), reducing shaping restrictions for differently characterized pulses. Additionally, the entire shaping process takes less than one minute [24]. This technology works in three stages, as shown in Figure 2. First, the femtosecond laser beam emitted from the laser is measured by the system as the reference phase

(with all distortions). After the initial pulse is measured by the spectrometer, the phase is calculated and recorded by the computer software. Finally, the process utilizes the initially recorded phase, and emits a complement phase to compensate for all imperfections/alterations until the "ideal" pulse is generated [21,24]. Shaped femtosecond laser pulses can also subject molecules to coherent control. Molecular coherence occurs when all molecules in a sample undergo similar dynamics simultaneously—that is, absorbing photons simultaneously resulting is unity in oscillation [25]. While coherence is presently known among pigment-molecule coupling during photosynthesis and diffraction grating in a vacuum [26], no current method exists to control coherence in the product channel—the products produced from reaction—in molecular dissociation.

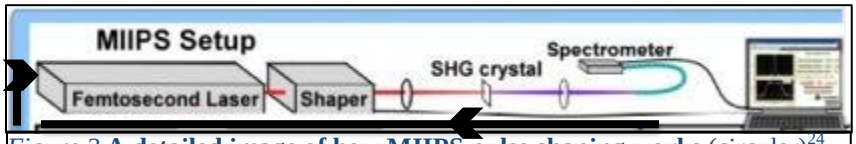

Figure 2 **A detailed image of how MIIPS pulse shaping works** (circular)[24]

Additionally, coherent control is the result of guiding the interaction between the laser and the matter via manipulating the phase of the pulse [27] when all particles of a sample undergo similar motion simultaneously. Coherent control makes possible controlled experiments in which researchers can subject the particles to a broad variety of alterations [25].

Triiodide

Equally important for the quality of the laser pulse is how the femtosecond pulse interacts with the sample being tested [28]. A preferable sample to test the interactions with femtosecond lasers is triiodide (I_3^-) [9,29,30]. This ion has a broad band of absorption, ranging from near UV to near-infrared (NIR) absorption, and has a very simple structure of three iodine atoms linearly single bonded (see Figure 3 A), making it a model that is easily testable under various conditions for the ease with which theories can be tested experimentally [9]. When I_3^- is

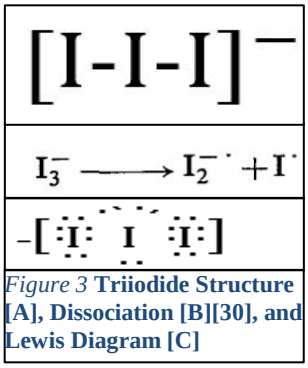

Figure 3 **Triiodide Structure [A], Dissociation [B][30], and Lewis Diagram [C]**

excited by the laser, it will photodissociate (split into components via light interactions) into diiodide and iodine (see Figure 3 B)[29]. After undergoing photodissociation, the nascent components of I_3^- follow patterns of coherent vibrations, thus causing oscillations in spectrum absorption. Since these vibrations often have very low frequencies, their vibrational coherence is easily observable via photon transmission scans [31]. However, these oscillations only last a few femtoseconds, as the particles quickly return to the ground state. Given the parameters of the vibrational dynamics, it is essential that the pulse duration lasts no more than a picosecond (10^{-12} s) in order to probe the molecular components in the excited state, while diiodide molecules are still vibrating [32]. Furthermore, another use of $I_3^-$is often in dye-sensitized solar cells (DSCs), in which the I_3^-directly photodissociates into the diiodide, which undergoes oscillations and coherent vibrations [33]. In these cells, the triiodide/iodide redox model is the most efficient and stable model to date [33]. The knowledge obtained using the triiodide model can potentially help optimize the efficiency of dye-sensitized solar cells.

This project had three key goals. The first goal was to use shaped femtosecond pulses to achieve excitation of triiodide and to study the vibrational oscillations described in the literature [31,32]. This was designed to test the initial model. The second goal was to study the effect of shaping of the ultrashort laser pump pulse on the vibrational oscillations. It was hypothesized that shaped femtosecond pulses can increase the signal intensity of energy emitted from the vibrational oscillations of diiodide once the optimal parameters for maximum oscillation amplification are achieved. The third goal was if able to maximize the energy of the diiodide molecules—the product from the dissociation reaction—it becomes possible are able to experimentally apply the theory of quantum mechanics [34] to study whether products of a chemical reaction can absorb and emit photons at unique frequencies. This would suggest that it is possible to create a wavepacket in the product channel of a chemical reaction.

METHODS

M1. GENERATION OF THE UV LASER PULSE SHAPER PATHWAY

Prior to testing, a time-intensive laser setup had to be created that enabled the emittance of both 400nm and 800nm light for the desired pump-probe system. These wavelengths were selected for their efficiency at being excited and

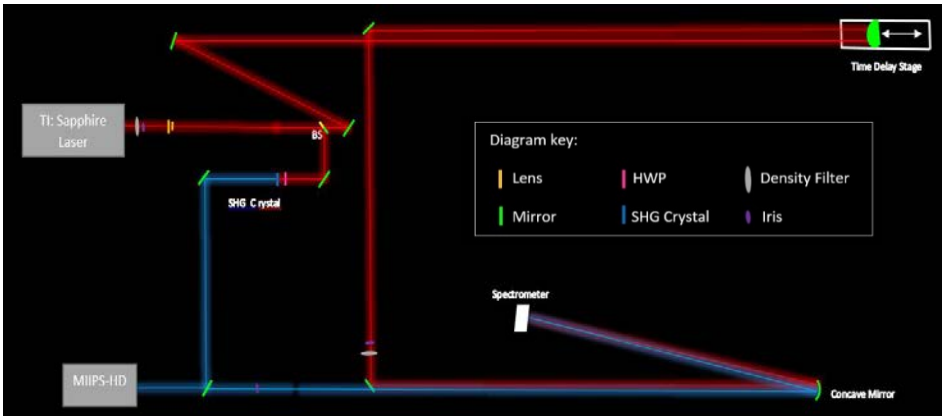

Figure 4a **Schematic: Determining the Optimal Pathway of the Laser beginning at laser and ending at spectrometer**

transmitted from the I_3^- and diiodide [32]. In order to do this, a Titanium-sapphire Laser system was utilized, which emits NIR (Near Infrared) light at ~800 nm. After traversing a series of lenses, mirrors, and density filters (which regulate intensity), the pulse interacted with a telescope, or two lenses that focus the beam to have a smaller circumference, followed by a beam splitter, which splits the 800 nm pulse into two pathways in a 90:10 ratio of intensity (see Figure 4a for a detailed pathway and part analysis of the laser setup). The 90 component then passed through a half wave plate, which flips the polarization, and a blue crystal, which ensures the cancellation of all non-blue light and re-flips polarization, creating second harmonic generation (SHG) of the initial pulse. This pulse, after undergoing SHG, had half the wavelength (400 nm) of the original pulse, and twice the frequency. This pulse then followed along a predetermined path into the MIIPS pulse shaper. Once it underwent shape characterization and correction, the emitted pulse was directed at a concave mirror. While the 400 nm pulse was being

shaped, the 10 component of the original beam was directed along an extensive path of mirrors and a moveable stage. While the composition of this beam (800 nm) remains unaltered, it was necessary that its path is elongated. Not only did the 800 nm and 400 nm pulses need to meet at the same point, but they also needed to travel the same distance in order to ensure that an error due to a time delay between the two pulses remains minimal. Of note, the stage allows 100 mm of movement.

This process required routine calibration and minuscule alterations to ensure precise distance measurements between the two pulse pathways that have no more than 1mm difference [17]. Additionally, three irises (small circles with holes aligned with the laser beam height) were utilized to ensure that despite any alterations to the system, an original pathway is always retained as a reference point for the ideal laser pathway. After travelling the necessary distance, the 800 nm pulse was then directed to the same concave mirror as the 400 nm pulse, and because of the converging effects of the mirror, the two interfere at a given point. While this interference does produce a pulse with a wavelength of 266 nm (UVA spectrum) [35]at time delay 0, a UV spectrometer was placed behind the sample to measure the resulting light to ensure accuracy. Once the system was set up, roughly 30 time delay scans were run to ensure the two beams interacted with the sample at the same time (to establish an accurate value without positive or negative time delay), and were continuously calibrated and rerun until an intense signal with a clear peak at time zero was present on the scan.

M2. Solutions and Reagents

A 3 mM solution of I_3^- was prepared by dissolving 0.7614 g of diiodide and .83 g of potassium iodide (KI) in 1000 mL spectroscopy grade ethanol, following the methods of Kliner et. al. [36]. However, since it is difficult to dissolve KI in ethanol, the KI crystals were first ground using a mortar and a pestle and heated in a sonicator bath while undergoing constant stirring. The solution was then placed into a 1mm flow cell cuvette, and connected to a liquid

pump which circulated the solution to prevent the laser from burning a hole (damaging the molecules from overexposure) through one part of the sample [37].

M3. Reproducing Oscillations Experimentation Setup

The experimental setup for the UV laser (Figures 4a and 4b) was utilized for experimentation. The actual physical setup of the laser system is shown in

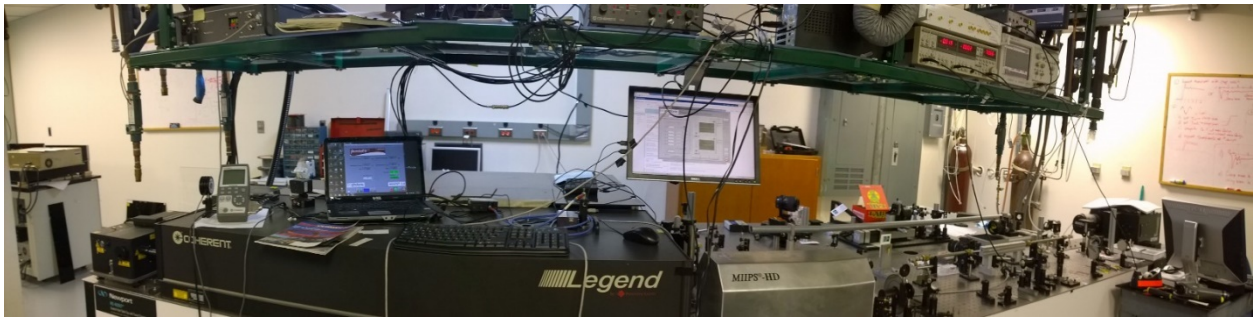

Figure 4b.

Figure 4b Photograph: **Determining the Optimal Pathway of the Laser—Physical Setup from laboratory**

The I_3^- flow cell was placed where the two pulses overlapped. Initially, the UV spectrometer was replaced with an NIR spectrometer to measure the emittance from the probe pulse. Later, a photodiode replaced the spectrometer because it is capable of detecting smaller changes in light intensity than a spectrometer, as it converts photons (i.e. light) into electrical current, which is then detected as a strong probe energy signal analogous to that observed with the spectrometer [38]. Next, a chopper—essentially a spinning propeller—was introduced between the pulse shaper and the spot at which the blue and red pulses travel parallel paths. The chopper was used to physically break up the pump pulse to ensure only the probe pulse signal is being amplified, as it reduces excess pump pulse present over larger time delays that could be detected inadvertently [39]. A lock-in amplifier was also used to further amplify the probe signal. Lock-in amplification is enabled by phase-sensitive detection which singles out the component of the signal at the correct frequency (in this case, the one associated

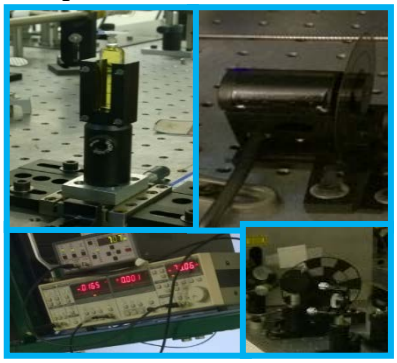

Figure 5: Close ups of constituents of the laser setup. A. The triiodide sample in the flow cell; B. The chopper in motion; C. The lock-in amplifier; D. The chopper still.

with the 800 nm) and also cancels out noise and any other detected light frequencies. Furthermore, normalized intensity vs. time delay scans (i.e. transient transmission scans) were then run on the sample, measuring the alterations in signal intensity (oscillations) as the sample was probed. This experiment was designed to reproduce the previously described oscillations [32].

M4. Analyzing Oscillation Periods

After running 50 transient transmission scans, the data were averaged into one graph (Figure 7). Using Excel, a new graph was generated that began after the increase in negative signal, and thus at the beginning of the oscillations. Next, the data were fitted to a fourth order polynomial, the line of best fit, showing the data had many fluctuations and bends [40]. This line most closely equated to the oscillation shape of the data without too high of an order. Following this, the 'x' values in the line of best fit were replaced with time delay data for each of the points to promote accuracy via the experimental value. The steps in creating the diidiodie oscillations along a flat line graph (Figure 8) are as follows:

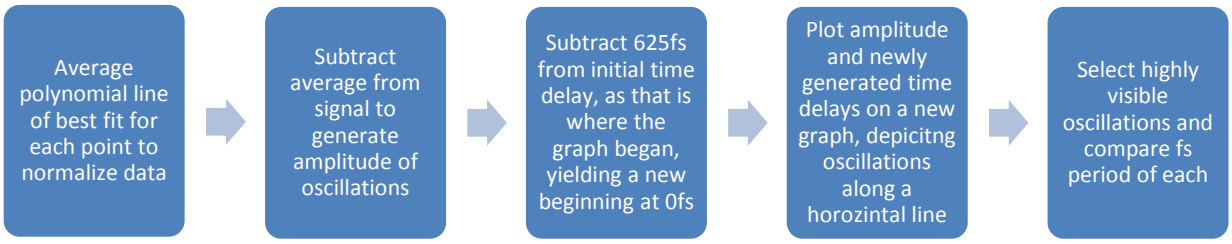

M5. Experimental Setup Maximizing Oscillation Amplitude

The triiodide sample was replaced with a fresh 3.0 mM I_3^- solution to ensure the sample's integrity. The same setup was utilized, replicating the setup used to measure vibrational oscillations. First, laser alignment, time delay scans, and spectrometer measurements were all completed to once again ensure the accuracy of the setup. Next, to maximize the oscillations, a transient transmission scan of the new sample was taken, as this would be the sample for further testing. At the second oscillation, the time delay of both the peak and valley were recorded, as they were far enough removed from the initial peak and valley to be misidentified as still initially rising, yet intense enough to not be mistaken for

noise. Then, utilizing the formula $distance = (velocity) * (time)$ (where "velocity" is the speed of light and "time" is the delay time), the distance the stage needed to be displaced in order to determinate positive and negative shifts was calculated for the peak and valley. The delay stage was moved to these positions, and then chirp (second order dispersion) scans were ran, as these display the position for maximized intensity for each component. The difference between the chirp scans (measured in fs^2) at the peak and valley positions were computed, and at this point, the difference demonstrated the optimal chirp value for scans that should indicate increased oscillation amplitudes.

RESULTS

Figure 6 **Setup and Calibration to read a UV Signal**

R1. Generation of the UV Laser Pulse

Laser setup optimization included minute calibration changes to ensure the optimal signal (centered over time delay zero and peaking at maximum signal intensity) was read. Time delay scans depicted the process of optimizing the UV signal at 266 nm (Figure 6a). In scan A, the seemingly flat line represents solely noise recorded at each time delay point. The time delay stage was programed to move up and down until the spectrophotometer detected signal. Scan B depicts

the signal detected initially, peaking at an intensity well below the optimum value. To compensate for this, the density filters used in the setup were opened, enabling more of the laser light to reach the point of overlap, thus increasing the intensity. The increased intensity can be seen in the scan C, specifically by the peak intensity value at roughly 190 arbitrary units (a.u.), which is close to the optimal intensity. Lastly, since experiments must be carried out with time zero being highly accurate, the stage was slightly adjusted once again to correlate the peak intensity at point zero, as depicted in scan D. Through this trial and error testing, a high intensity 266 nm UV laser signal was produced from the experimental setup, as shown.

R2. Reproducing Oscillations

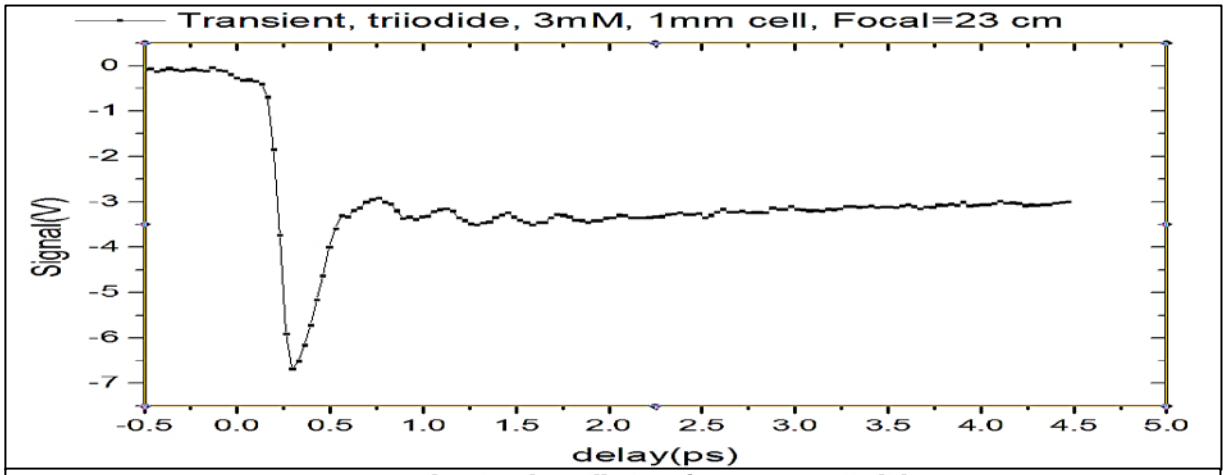

Figure 7 **Vibrational Oscillations from 3mM Triiodide**

Initially, the triiodide solution scans did not show any oscillations. To remedy this, a lock-in amplifier was added to the setup, and a signal was generated. An averaging factor was implemented on the computer scan, taking 151 measurements during scanning. Fifty transient transmission scans were ran, averaged, and plotted. In Figure 7, the transient transmission scan shows that at the time delay zero, UV light begins to cause the triiodide to dissociate, as indicated by the sudden dip (.2ps-.3ps), producing diioidide. Then, the diiodide absorbs the probe pulse of 800nm. The oscillations correspond to diiodide

vibrational motion, prominent between .5ps and 2ps, and tappers off at 4ps. Since oscillations were present in the .5ps-2ps range, it was validated that vibrational oscillations can be successfully reproduced. Furthermore, upon comparison of these oscillations to those produced by Vöhringer [32], the general shapes and timing on scans revealed much similarity, thus ensuring that the initiation of the oscillation period and maximization analysis of the experiment were conducted with a valid model.

R3. Analyzing Oscillation Period

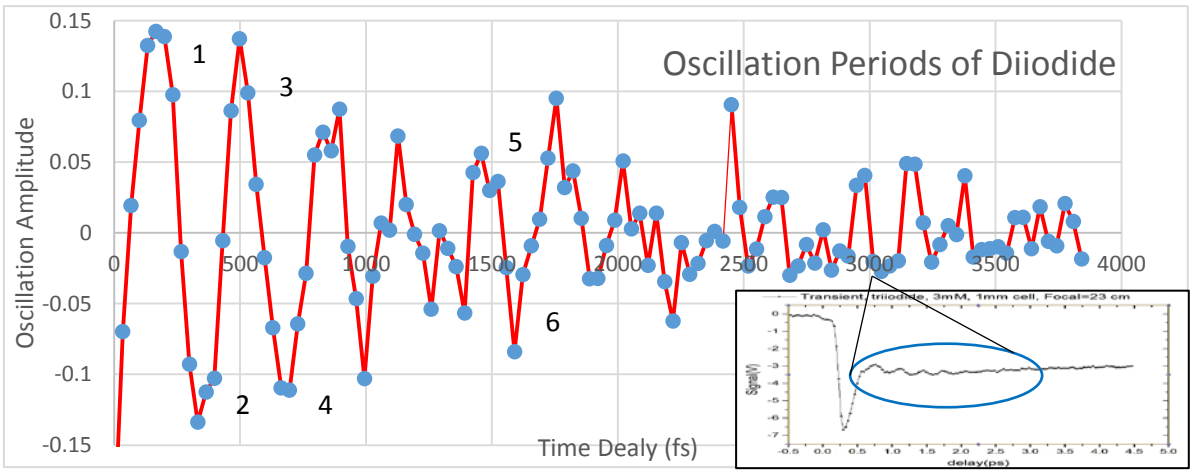

Figure 8 **Interpreting oscillation periods of Diiodide**

Figure 7 Minimized for reference; Enlargement allowed for conversion of picoseconds to femtoseconds.

In order to analyze the oscillation period over time, which provides information on the changing rate of reaction, the vibrational oscillations depicted in Figure 7 from .5ps-4ps were normalized to a horizontal line graph in Figure 8. Before calculations of oscillation period could be recorded, differentiation between oscillation and noise had to be determined. Selected oscillations were chosen for their prominence and clarity in peak-to-peak shape to ensure that data included only signal and minimal noise. Furthermore, these oscillations did not include oscillation direction shifts, as seen around 1300 fs. Once the six desired oscillations (depicted in Figure 7) were chosen for

Oscillation Number (L-R)	Beginning X	Ending X	**Oscillation Period (fs)**
1	166	498	**332**
2	365	696	**331**
3	498	828	**330**
4	696	994	**298**
5	1458	1756	**298**

Table 1 **Oscillation Periods of diiodide**

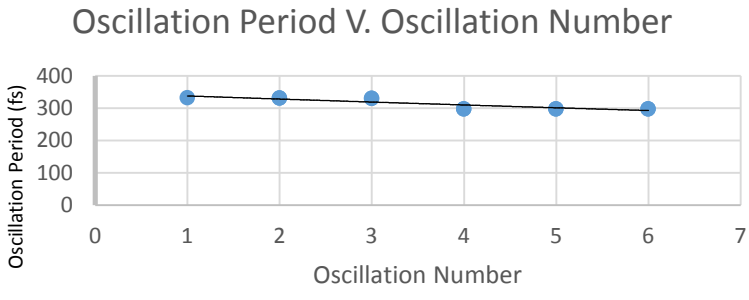

Figure 9 **Monitoring Alterations in Oscillation Period**

measurements, the difference between the beginning and end data point (on the x-axis of time delay) for each oscillation was calculated. Duration of oscillations expressed in fs (Table 1) showed oscillation effects over time.

Table 1 and Figure 9 depict a steady decrease in oscillation period. The first oscillations have periods of 333fs, while the latter ones last 298fs. This trend suggested that the reaction oscillation is getting faster. This trend is also interesting, because it shows that diiodide fragments oscillated faster as they cool. This is because the potential energy that is responsible for the oscillations is not harmonic. At high energies, the energy of the bond gets slightly weaker, for the thermal energy exceeds the potential energy of the bond [36], thus reducing activation energy and making the reaction occur faster.

R4. Interpreting Molecular Coherence (Quantum Physics)

In order to understand that quantum laws (viewing light as particles) are applied in the oscillations and that coherence (all of the particles exhibiting similar behaviors simultaneously) was being observed, it was mathematically determined that there was an adequate number of photons to interact with the molecules present. In order to do this, first, the number of molecules was computed, given the cuvette volume of $1mm^3$ and the concentration of solution being 3 mM, as follows:

Volume: $1mm^3 = 1x10^{-6}L$

Solution molarity: $3x10^{-3}M/L * 1x10^{-6}L = 3x10^{-9}M$

Number of molecules: $3x10^{-9}M * 6.02x10^{23} = 1.81x10^{15} molecules,$

Assuming only 1% of the molecules in solution undergo coherence, as the beam only focuses on a very small portion of the entire cuvette, then:

Potential number of molecules undergoing coherence: $1.81x10^{15} * .01 = 1.81x10^{13}$

Once the predicted number of molecules undergoing coherence was computed ($1.81x10^{13}$), it was necessary to determine the number of photons

available to ensure that this number of molecules could be excited by the amount of light energy yielded in the experiment:

Energy of produced photons in reaction:

$$E = \frac{hc}{\lambda} = \frac{(6.6x10^{-34}J/s)(3.0x10^{8}m/s)}{400x10^{-9}m} = 4.95x10^{-19}J$$

Then, assuming that the laser was functioning properly at approximately 1mW with a repetition rate of 1000W/s, the pump pulse energy is roughly $1x10^{-6}J$. Given this, it can be determined the number of photons in the entire reaction:

$$\frac{Energy\ of\ pump\ pulse}{Energy\ of\ one\ photon} = \frac{1x10^{-6}J}{4.95x10^{-19}J} = 4.95x10^{13}\ \text{photons}$$

It must be taken into consideration that all of these photons are not used in the reaction, as the UV pulse can still be detected post-interaction with the sample, suggesting that there are still photons unused in reaction. Then, upon comparison of the number of molecules ($1.81x10^{15}$) to the number of photons used ($4.95x10^{13}$), it can be concluded that there are enough photons to excite a large number of molecules, thus validating the quantum nature of coherence. This is of immense significance, for not only does it show that the excited molecules do spontaneously emit photons to produce a coherent light source, but it also signifies the ability to apply quantum theory to experimental reactions.

R5. Maximizing Oscillation Amplitude

Chirp scans were generated by imposing a second order dispersion factor on the pulse shaper program for the pump pulse in attempt to decrease dispersion effects upon entering the sample, generating the optimal pulse for further testing.

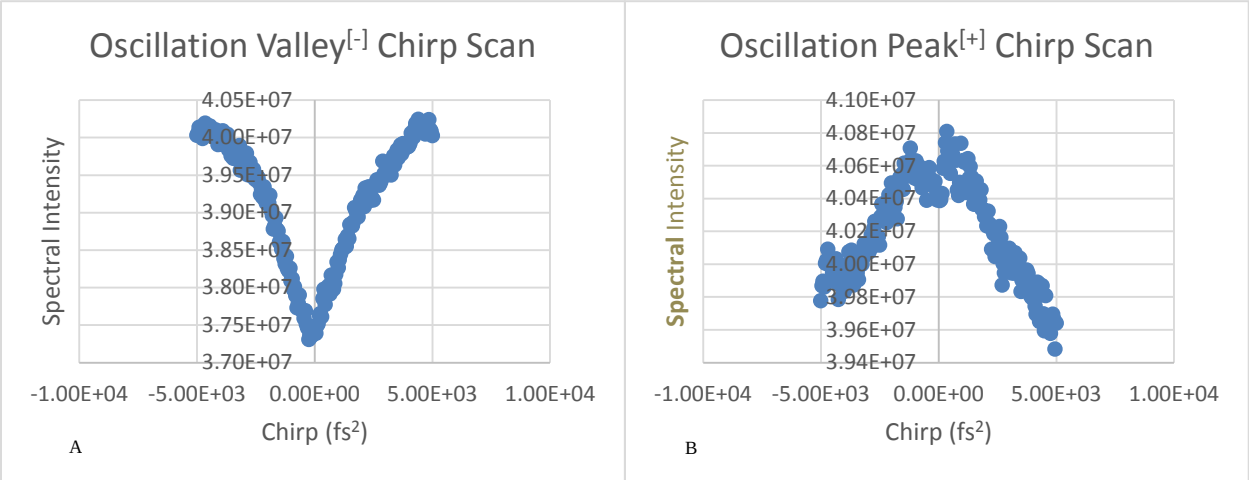

Figure 10 **Oscillation Valley and Peak Chirp Scans**

The data from the peak and valley chirp scans were compared in Figure 10. In these scans, second order dispersion shaping parameters were applied to the pump pulse. After analyzing the negative chirp scan (Figure 10A), it is evident that the maximum intensity of the laser is present not at a transform-limited (minimally altered) pulse, but rather at one with second order dispersion and a slightly negative time delay imposed between the pump and probe pulses, as indicated by the tip of the "v-shape" shifted to the left of the zero chirp mark. Contrarily, Figure 10B shows that the maximum signal intensity for oscillation peak amplitude is found slightly positive of the zero chirp once second order dispersion is imposed. Since neither scan is optimized at zero chirp, this suggests that the optimal intensity is found at some other second order dispersion value not centered at the zero chirp. To determine this ideal point via subtraction of the two scans, it becomes evident that the ideal chirp for the maximized oscillatory amplitude is not at the zero alteration state, when the pulse is transform limited, but rather slightly shifted (chirped) at approximately ±1.0E2 fs^2. These maximized peaks and valleys (amplitudes), would provide a clearer, stronger

signal to test with maximized oscillation amplitudes once optimal chirp is deduced, consequently amplifying the energy yield from the photon emittance.

CONCLUSION

The presence of coherent vibrational oscillations of the diiodide molecules following dissociation demonstrates the quantum nature of the experimentally produced oscillations and the ability to manipulate energy generation in the product channel of a reaction. This study supports this presumed quantum nature, as the number of molecules that could undergo coherence versus the number of available photons produced to excite the molecules are roughly equal. This suggests that the photons of light in the laser pulse are indeed interacting with the molecules, and that the photons must be of a discrete energy frequency to maximize signal intensity of energy emittance.

Furthermore, while produced oscillations were comparable to those produced by Vöhringer [32], they were not nearly as intense. After an in-depth literature review, it was determined that utilization of an 800 nm probe pulse falls between the maximum in-phase and out of phase oscillations of 850 nm and 676 nm[32], thus producing oscillations with smaller amplitudes. Additionally, these results indicate that the excited molecules may undergo vibrational cooling at increased time delay, as the determined periods fall above the accepted minimum value. These results also suggest that cooling effects may take place, although additional experiments with increased number of scans, longer duration, and an increased signal-to-noise ratio are needed to validate the presence of vibrational cooling.

The fact that pulse-shaping constraints can be placed upon the pulses that made up the UV desired pulse at time zero demonstrates that the MIIPS pulse shaper can be successfully adapted to shape ultrashort UV pulses. Moreover, these data demonstrate that the oscillations may be amplified once the optimal chirp value is deduced. These results demonstrate a proof-of-principle of a

concept that a wavepacket in the product channel of a reaction can be focused. In summary, these data extend our knowledge of light-matter interaction, how quantum theory can be applied and tested experimentally, and improve the technology to control chemical reaction using ultrasort shaped laser pulses, which has significant commercialization potential.

The key findings of this study are:

- Quantum mechanics theory can be assumed the model by which coherence dynamics are observed within light-matter interactions.
- Photons of a discrete energy and the molecules that absorb and emit them in the product channel of a reaction can create an optimal energy yield at specific frequencies.
- The MIIPS pulse shaper can be used to shape a UV pulse.
- Molecular oscillations in diiodide appear to undergo cooling effects.
- Given difference maximum chirp values, there is a potential to increase the oscillation amplitude with a specific chirp value.

ACKNOWLEDGEMENTS

Special thank you to: the High School Honor Science Program at Michigan State University, Research advisor and director Dr. Gail Richmond for her continued support and guidance; Dr. Marcos Dantus, the head of the lab for his time; graduate students Anton Ryabtsev and Gennady Rasskazov for their assistance; my school research coordinator Ms. Mary Lou O'Donnell for providing me with invaluable foundation research skills; my parents for encouraging me in my research endeavors; and finally the NYSSEF board for selection and opportunity to publish my work in this High School Research Journal.

REFERENCES

[1] "Chapter 3: Control of Chemical Reactions." Opportunities in Chemistry. Washington, D.C.:National Academy, 1985. N. pag. Print.
[2] Sheldon, Roger A. "Fundamentals of Green Chemistry: Efficiency in Reaction Design." Chem. Soc. Rev. 41.4 (2012): 1437-451. Web.
[3] Anastas, Paul, and Nicolas Eghbali. "Green Chemistry: Principles and Practice." Chem. Soc.Rev. 39.1 (2010): 301-12. Web.
[4] National Research Council (US) Committee on Prudent Practices in the Laboratory. "Prudent Practices in the Laboratory: Handling and Management of Chemical Hazards: Updated Version." Management of Chemicals. U.S. National Library of Medicine, 2011. Web.
[5] Shapiro, Moshe, and Paul Brumer. "Principles of the Quantum Control of Molecular Processes." SAO/NASA ADS (2003): n. pag. Web.
[6] Noll, Walter. "The Foundations of Classical Mechanics in the Light of Recent Advances in Continuum Mechanics." Studies in Logic and the Foundations of Mathematics The Axiomatic Method (1959): 266-81. Web.
[7] Magyar, G., and L. Mandel. "Interference Fringes Produced by Superposition of Two Independent Maser Light Beams." Nature 198.4877 (1963): 255-56. Web.
[8] Chow, Tai. Mechanics, Second Edition. 2nd ed. Boca Raton: CRC, 2013. Print.
[9] Baratz, Adva, and Sanford Ruhman. "UV Photolysis of I3- in Solution – Multiple Product Channels Detected by Transient Hyperspectral Probing." Chemical Physics Letters 461.4- 6 (2008): 211-17. Web.
[10] Träger, F. "Chapter 1: Nonlinear Optics." Springer Handbook of Lasers and Optics. New York: Springer, 2007. N. pag
[11] Rosker, M. J., M. Dantus, and A. H. Zewail. "Femtosecond Clocking of the Chemical Bond." Science 241.4870 (1988): 1200-202. Web.
[12] Free University of Berlin. "Chapter 2: Femtosecond Laser Pulses." Berlin: n.p., 2015. N. pag. Web
[13] Trebino, R. Frequency-resolved Optical Gating: The Measurement of Ultrashort Laser Pulses. Boston: Kluwer Academic, 2000. Print.
[14] "The Future of Ultrashort Laser Pulses." Phys.org. Max Planck Society, 24 July 2014. Web.
[15] Gedik, Nuh. "Experiments." Mit.edu. Gedik Group, 2013. Web.
[16] Dorow, Chelsey. An Introduction to the Technique and Applications of Pump-Probe Spectroscopy. Rep. Physics.ucsd.edu, 2014. Web.
[17] Mimoun, Emmanuel, Luigi Sarlo De, Jean-Jacques Zondy, Jean Dalibard, and Fabrice Gerbier. "Sum-frequency Generation of 589 Nm Light with Near-unit Efficiency." Opt. Express Optics Express 16.23 (2008): 18684. Web.
[18] Agostinelli, J., G. Harvey, T. Stone, and C. Gabel. "Optical Pulse Shaping with a Grating Pair." Appl. Opt. Applied Optics 18.14 (1979): 2500. Web.
[19] Tomizawa, H., H. Dewa, and H. Hanaki. "Development of Automatically Optimizing System of Both Spatial and Temporal Beam Shaping for UV-laser Pulse." Laser Optics (2004): n. pag. Web.
[20] "Pulse-Shape Filtering in Communications Systems." National Instruments. N.p., 5 Nov. 2014. Web.
[21] Dantus, Marcos, Vadim Lozovoy, and Igor Pastrik. "MIIPS Characterizes and Corrects Femtosecond Pulses." Laser Focus World. N.p., 1 Jan. 2007. Web.
[22] Kazarinov, R., and C. Henry. "Second-order Distributed Feedback Lasers with Mode Selection Provided by First-order Radiation Losses." IEEE Journal of Quantum Electronics IEEE J. Quantum Electron. 21.2 (1985): 144-50. Web.

[23] Dantus, Marcos. "Laser Science to Photonic Applications." Proc. of CLEO:2015, San Jose Convention Center, San Jose. N.p.: n.p., 2015. N. pag. Print.
[24] Dantus, Marcos. "Automated Pulse Compression and Shaping for Ultrafast Lasers." Biophotonic Solutions Inc. N.p., n.d. Web. 10 July 2016.
[25] Fielding, Helen. "Coherent Control." Editorial. JOURNAL OF PHYSICS B: ATOMIC, MOLECULAR AND OPTICAL PHYSICS 2008: n. pag
[26] Arndt, Markus, Thomas Juffmann, and Vlatko Vedral. "Quantum Physics Meets Biology." HFSP Journal 3.6 (2009): 386-400. Web.
[27] He, Z.-H., B. Hou, V. Lebailly, J.a. Nees, K. Krushelnick, and A.g.r. Thomas. "Coherent Control of Plasma Dynamics." Nature Communications Nat Comms 6 (2015): 7156. Web.
[28] Wang, Weining. Femtosecond Spectroscopic and Molecular Dynamics Simulation Studies of Chemical Reaction Dynamics in Condensed Phases. Diss. Massachusetts Institute of Technology, 1995. N.p.: n.p., n.d. Print.
[29] Banin, Uri, and Sanford Ruhman. "Ultrafast Photodissociation of I3. Coherent Photochemistry in Solution." The Journal of Chemical Physics J. Chem. Phys. 98.6 (1993): 4391. The Journal of Chemical Physics. Web.
[30] Gilch, Peter, Ingmar Hartl, Qingrui An, and Wolfgang Zinth. "Photolysis of Triiodide Studied by Femtosecond Pump−Probe Spectroscopy with Emission Detection." J. Phys. Chem. A The Journal of Physical Chemistry A 106.9 (2002): 1647-653. Web.
[31] Banin, Uri, and Sanford Ruhman. "Ultrafast Vibrational Dynamics of Nascent Diiodide Fragments Studied by Femtosecond Transient Resonance Impulsive Stimulated Raman Scattering." The Journal of Chemical Physics J. Chem. Phys. 99.11 (1993): 9318. Web.
[32] Kühne, Thomas, and Peter Vöhringer. "Vibrational Relaxation and Geminate Recombination in the Femtosecond-photodissociation of Triiodide in Solution." The Journal of Chemical Physics J. Chem. Phys. 105.24 (1996): 10788. Web.
[33] Boschloo, Gerrit, and Anders Hagfeldt. "Characteristics of the Iodide/Triiodide Redox Mediator in Dye-Sensitized Solar Cells." Accounts of Chemical Research Acc. Chem. Res. 42.11 (2009): 1819-826. Web.
[34] Squires, Gordon Leslie. "Quantum Mechanics." Encyclopedia Britannica Online. Encyclopedia Britannica, 17 June 2016. Web.
[35] Mimoun, Emmanuel, Luigi Sarlo De, Jean-Jacques Zondy, Jean Dalibard, and Fabrice Gerbier. "Sum-frequency Generation of 589 Nm Light with Near-unit Efficiency." Opt. Express Optics Express 16.23 (2008): 18684. Web.
[36] Kliner, Dahv A. V., Joseph C. Alfano, and Paul F. Barbara. "Photodissociation and Vibrational Relaxation of I2− in Ethanol." The Journal of Chemical Physics J. Chem. Phys. 98.7 (1993): 5375. Web.
[37] J. Haas, R. Stach, M. Sieger, et al., Anal. Methods. (2016)
[38] Nave, Rod. "Photodiode Light Detector." Photodetectors. Georgia State University, 2000. Web.
[39] Stanford Research Systems. Model SR830 DSP Lock-In Amplifier. Sunnyvale: n.p., 2011. Print.
[40] "Choosing the Best Trendline for Your Data." Microsoft Office Support. Microsoft Corporation, 10 Sept. 2016. Web.